VOx/Al2O3 Catalyzed Oxidative Dehydrogenation of Propane: Focus on Catalyst Characterization and Deactivation Behavior

Francisco Passamonti, Silvana D'ippolito, María Vicerich, María Sanchez, Sonia Bocanegra, Nadia Guignard, Catherine Especel, Florence Epron, Carlos Pieck, Viviana Benítez

VO_X/Al_2O_3 catalyzed oxidative dehydrogenation of propane: focus on catalyst characterization and deactivation behavior

Francisco J. Passamonti[1], Silvana A. D'Ippolito[1], María A. Vicerich[1], María A. Sanchez[1], Sonia Bocanegra[1], Nadia Guignard[2], Catherine Especel[2], Florence Epron[2*], Carlos L. Pieck[1], Viviana M. Benítez[1*]

[1]Instituto de Investigaciones en Catálisis y Petroquímica (INCAPE, UNL-CONICET), Colectora Ruta Nac. Nº 168 - Paraje El Pozo, Santa Fe, Argentina.

[2]CNRS, Université de Poitiers, Institut de Chimie des Milieux et des Matériaux de Poitiers (IC2MP), F-86000 Poitiers, France.

Corresponding authors:

Florence Epron

IC2MP B27

4 rue Michel Brunet

TSA 51106

86073 Poitiers Cedex 9, France

Tel. + 33-5-49454832

E-mail: florence.epron@univ-poitiers.fr

Viviana Monica Benitez

INCAPE

Colectora Ruta Nac. Nº 168 Km. 0 - Paraje El Pozo

3000 Santa Fe, Argentina

Tel. +54-342-4511370

E-mail: vbenitez@fiq.unl.edu.ar

Abstract

Oxidative dehydrogenation of hydrocarbons (ODH) converts propane and/or ethane into propylene and/or ethylene, which are important compounds in the chemical industry. Unlike steam cracking, ODH offers high theoretical conversion to olefins and lower energy consumption. The ODH reaction of propane to propylene was studied using VO_X/Al_2O_3 catalysts prepared by wet impregnation. The reaction conditions were widely varied, with temperatures ranging from 300 ºC to 550 ºC, the C_3/O_2 ratio from 1.6 to 3.3 and the vanadium content from 1 to 11 wt%. It was observed that these parameters are key experimental variables that influence the performance of the catalysts in ODH. Catalysts with intermediate vanadium loading exhibit an optimal amount of acidic sites due to the presence of monomeric and polymeric VO_X species, resulting in high selectivity towards propylene. Temperature programmed oxidation analyses showed that coke deposition is proportional to the degree of VO_X polymerization.

Keywords: ODH, propane, propylene, VO_X/Al_2O_3, deactivation

1. Introduction

The term "light olefins" includes mainly ethylene and propylene. Both olefins are widely used for the production of plastics, fibers and many other chemical products such as oxygenated compounds (ethylene glycol, acetaldehyde, acetone, propylene oxide, etc.) and intermediate products (ethylbenzene, propionaldehyde, etc.). These derived materials find applications in a variety of industries, such as textiles, automotive, packaging, and construction [1, 2].

Currently the leading technology for the production of olefins is steam cracking (SC). This is a complex process that produces a wide range of products and is versatile in terms of the feedstock used, ranging from light hydrocarbons such as ethane, propane and butane, to naphtha and distilled fuel oil. However, the recent shift in raw material feedstock to shale gas, which contains a large amount of ethane, has led to lower propylene yields in these processes, creating a growing gap between propylene supply and demand. To reduce this gap, there is increasing industrial interest in producing propylene from propane [3]. However, this demand cannot be met by the traditional SC process due to the low propylene/ethylene ratio obtained. To address this issue, several alternatives have been proposed, but these must be economically viable and comparable to current SC units in terms of production capacities. Additionally, it is important to note that the SC process is the most energy-intensive process in the chemical industry. Worldwide it consumes approximately 8% of the sector's total primary energy use, excluding the energy required for final products manufacturing [4]. Furthermore, it is essential to highlight the significant CO_2 emissions that this process generates worldwide [4]. Reducing these emissions is a crucial aspect from an environmental point of view.

The current alkane conversion technology, based on the dehydrogenation process, has several disadvantages, such as high endothermicity, unfavorable equilibrium shift and

difficult control of cracking side reactions at high temperatures, which contribute to the rapid coking of the catalyst [5-7]. Therefore, the alternative conversion route consisting in the oxidative dehydrogenation (ODH) process becomes promising.

The oxidative dehydrogenation of propane (ODHP) in the presence of molecular O_2, as an oxidizing agent, promotes reactions at low temperatures and is exothermic without thermodynamic limitations [8]. A major challenge in the commercial development of ODHP is improving propylene yields, as significant oxygenated by-products are formed. The primary cause of the selectivity limitation arises from the conversion-selectivity relationship; an increase in conversion results in a decrease in propylene selectivity [9, 10]. Specifically, in the oxidative dehydrogenation of propane to propylene, selectivity to propylene at higher propane conversion is limited by the adsorption of propylene on the acidic sites of the catalyst and its subsequent combustion to carbon oxides [11]. Different catalysts have already been studied in ODHP, including those containing V, Mo, Cr, Pt and Ga supported on zeolites, TiO_2, SiO_2 and Al_2O_3 [12-14].

VO_X-supported catalysts are among the most promising because they demonstrate good on-stream stability and high selectivity [15]. However, the structure of supported VO_X-based catalysts is very complex, and the structure-performance relationship of VO_X-based catalysts has been the subject of many studies for propane dehydrogenation reaction [13] and ODHP [9]. For ODHP, the polymeric or crystalline species favor the deep oxidation process of propylene into CO_2. The most widely accepted hypothesis regarding the process involved in the ODH reaction is the Mars van Krevelen (MvK) mechanism, in which the catalyst undergoes a cycle of reduction and oxidation, while the reactants are simultaneously converted into the products [9, 16]. However, the reaction mechanism depends strongly on the catalyst composition. On VO_X/Al_2O_3, it was proposed that, for the ODH of ethane, a combined mechanism is involved, where ethane is produced by

dehydrogenation through MvK mechanism. In that case the activity strongly depends on the ability of V to change its oxidation state, but the oxidation is governed by a Langmuir-Hinshelwood (LH) mechanism involving one single active site and the competitive adsorption of the reactants. The challenge in this reaction is to develop catalysts that are not only active at relatively low temperature and resistant to deactivation, but also capable of preventing the undesirable oxidation reaction of propylene to CO_X products.

While the role of the nature of the VO_X species was still unclear, it was recently demonstrated for non-oxidative propane dehydrogenation, that VO_X aggregates in the form of low-polyvanadate presented better activity and stability than isolated VO_X species and highly polymerized species as V_2O_5. Various VO_X species were obtained by varying the V loading in hexagonal mesoporous SiO_2 (HMS) [17]. However, the HMS support does not exhibit acidity, and facilitates the metal dispersion due to its specific structure, both of which help limiting the deactivation. This raises the question: are the same low-polymerized VO_X species the most active and stable when the reaction is performed in the presence of oxygen and when a classical alumina support is used?

To address this question, one of the objectives of this work was to investigate the influence of the physicochemical properties of VO_X catalysts on their catalytic performance in ODHP, using a classical γ-Al_2O_3 support, by varying the kind of VO_X species following the strategy used in [17], i.e., by varying the V content in a wide range (from 1 to 11 wt.%). For this purpose, catalysts were prepared by the wet impregnation method in aqueous medium of vanadium precursors using γ-Al_2O_3 as support. Several analytical techniques (ICP-OES, N_2-physisorption, XRD, TPR, Raman spectroscopy, SEM, XPS and TPD-Py) were used to study the distribution and arrangement of vanadium species on the γ-Al_2O_3 support.

Besides the characterization of the catalytic materials, their activity and selectivity for the ODHP reaction were evaluated under different conditions: several propane/dioxygen ratios

in the feed and reaction temperatures. Temperature programmed oxidation (TPO) was performed to characterize the carbon deposit after catalytic test.

2. Experimental

2.1. Catalyst preparation

Five vanadium samples supported on γ-Al_2O_3 were prepared using the wet impregnation method. NH_4VO_3 (CAS number 7803-55-6, Merck ACS reagent, ≥ 99.0%) in aqueous medium (50 ml) was utilized to achieve a final vanadium content within the range of 1.0% to 11.0% by weight. 5 g of γ-Al_2O_3 support (Cyanamid Ketjen CK-300, pore volume of 0.5 cm^3 g^{-1}, specific surface Sg of 180 m^2 g^{-1}, and a particle size range of 35–80 mesh) was previously calcined at 450 ºC. Finally, the mixture was stirred at a temperature ranging from 55-60 ºC for 2 h. The resulting solid product was subsequently dried in an oven during 12 h at 120 ºC, followed by calcination in air using a heating rate of 5 ºC min^{-1} from room temperature to 500 ºC and maintained at this temperature for 4 h. Samples were sieved to 35-80 mesh particle diameters. The impregnated samples were identified as V(x)/Al, with "x" being the expected weight content of vanadium.

2.2. Catalytic test

The evaluation of the catalytic activity in the oxidative dehydrogenation of propane (C_3) was performed at ambient atmospheric pressure using a quartz tube reactor (ID = 4 mm) equipped with a fixed bed and 100 mg of catalyst confined between quartz wool (without diluents), generating a catalytic bed of 8 mm high. Samples were heated from room temperature to reaction temperature (300 ºC, 350 °C, 400 ºC, 450 °C or 550 °C) under air flow (30 ml min^{-1}, 10 ºC min^{-1} ramp). Temperature control was maintained using a K-type thermocouple positioned between the furnace and the reactor, at the height of the catalytic

bed. The C_3/O_2 ratio was varied from 1.6 to 3.3 (10, 15 and 20 cm^3 min^{-1} C_3 flow, keeping constant the O_2 flow at 6 cm^3 min^{-1}) and 24 cm^3 min^{-1} N_2 flow (total flow: 40, 45 or 50 cm^3 min^{-1}). The products were analyzed using a Shimadzu GC-2014 with a TCD detector and Carbosieve adsorbent S-II 80-100 mesh (Supelco) column for CO and CO_2 analysis, and Thermo Scientific Trace 1300 GC with FID detector and ZB-1 capillary column for C_1–C_4 hydrocarbons. To make the two chromatographic analyzes compatible, an internal standard (cyclohexane) was added, which eluted completely separated from the other compounds. Additionally, experiments were carried out with lone γ-Al_2O_3 under the same reaction conditions.

Turn-over frequency (*TOF* in s^{-1}), conversion (*conv*%) and propylene selectivity (Sel_i %) were determined using Equations (1-3):

$$TOF = \frac{F_{C_3}.conv.MW_V}{w_{cat}.c} \quad (1)$$

$$conv\ \% = \frac{w^{in}_{C_3H_8} - w^{out}_{C_3H_8}}{w^{in}_{C_3H_8}} 100 \quad (2)$$

$$Sel_i\ \% = \frac{w_i}{w^{in}_{C_3H_8} - w^{out}_{C_3H_8}} 100 \quad (3)$$

where:

F_{C_3} : propane flow (mol s^{-1}).

$conv$: conversion (%).

MW_V : vanadium molar mass (g mol^{-1}).

w_{cat} : catalyst mass (g).

c: percentage (%) of vanadium in surface of the catalyst given by XPS, except for V(1)/Al, where c is the real V content determined by ICP.

$w_{C_3H_8}^{in}$: mass of the propane at reactor inlet (g).

$w_{C_3H_8}^{out}$: mass of propane in the outlet of the reactor (g).

w_i: mass of the product (*i)* in the outlet of the reactor (g).

2.3. Catalysts characterization

The V content of the catalysts was determined by ICP-OES after digestion in an acid solution. The equipment used was Perkin Elmer Optima 2100 DV.

A Micromeritics ASAP 2020 instrument was used to perform N_2 adsorption-desorption measurements. For analysis, 300 mg of samples were degassed at 200 °C for 8 h. BET surface areas were obtained using the Brunauer-Emmett-Teller (BET) and the pore volume and diameter determination using Barrett-Joyner-Halenda (BJH) method.

X-ray diffraction (XRD) analyzes were conducted at room temperature on a Panalytical diffractometer. The monochromatic Cu Kα radiation (λ = 1.54 Å) was used. The diffractograms were recorded in the 2θ range from 5 to 80° with a step of 0.05º.

Laser Raman spectroscopy (LRS) analyzes were performed at room temperature with a HORIBA Jobin Yvon Labram HR 800 UV Raman confocal microscope equipped with a Peltier-cooled CCD detector. The excitation wavelength of 532 nm is produced by an external laser diode (Oxxius). The spectrometer is attached to a confocal microscope equipped with an Olympus 100x planar objective (N.A. 0.90). LabSpec 5 software allows acquisition and processing of results.

A benchtop scanning electron microscope (SEM) Phenom-World PROX operating at 15 kV equipped with an energy dispersive X-ray spectrometer (EDS) was used for the

morphological characterization and for elemental analysis/mapping. The powder material was dispersed and fixed onto a SEM pin stub with a double-sided graphite tape. A charge-reduction sample holder for non-conductive samples was employed in all SEM characterizations.

Pyridine temperature-programmed desorption (TPD-Py) profiles were measured using an FID detector. Pyridine was adsorbed on 200 mg of samples at room temperature; the physisorbed pyridine was removed at 110 °C for 1 h under a nitrogen flow (40 cm^3 min^{-1}). The temperature was then varied from 110 °C to 650 °C. Calibrated pulses of pyridine were used to determine the amount desorbed from the catalysts [18].

The X-ray photoelectron spectroscopy (XPS) measurements were recorded using a Kratos Axis Ultra DLD equipment with a monochromatic Al X-ray source (1486.6 eV, 10 mA, 15 kV). The spectra were obtained with a pass energy of 20 eV on an analysis area of 300 μm×700 μm. The spectral region corresponding to V 2p core levels was recorded for each sample. Data were acquired with 0.1 eV steps. The calibration of the spectra was performed with the Al 2p line (74.4 eV) of γ-Al_2O_3 support. The data treatment was performed with the Casa XPS program.

The temperature-programmed reduction (TPR) experiments were carried out in a AutoChem 2920 equipment by heating 150 mg of sample, at heating rate of 10°C min^{-1}, from 30 to 800 °C, under 30 cm^3 min^{-1} flow of a 5%H_2/N_2 mixture, after a pretreatment under air (1 h, 500 °C).

The carbon deposits on the surface of the catalyst were analyzed by means of temperature-programmed oxidation (TPO). 25 mg of the coked catalyst was placed in a quartz glass reactor. The carbon was then burned by an oxidizing stream (60 cm^3 min^{-1} flow of 5%O_2/N_2 mixture). The temperature of the cell ramped from 30 to 700 ºC at a constant rate of 10 ºC

min^{-1}. Exhaust gases were fed to a methanizer where CO_2 and CO were converted to CH_4 with a Ni catalyst in presence of H_2. The resulting CH_4 stream was detected by a FID.

3. Results and discussion

3.1. Characterization

Table 1 presents the vanadium content ascertained via ICP-OES analysis, and the textural properties measured by N_2 physisorption for prepared samples after calcination.

Table 1: Vanadium loading (measured by ICP analysis), BET surface area, pore size (Dp), and pore volume (Vp) of the catalysts.

Catalyst	Vanadium loading, wt%	BET surface area, $m^2\ g^{-1}$	Dp, Å	Vp, $cm^3\ g^{-1}$
V(0)/Al	0	180	77.4	0.47
V(1)/Al	1.2	178	77.7	0.48
V(3)/Al	3.0	161	79.2	0.43
V(6)/Al	5.4	156	74.3	0.40
V(9)/Al	8.8	143	77.9	0.37
V(11)/Al	10.4	137	78.1	0.36

The specific surface area and total pore volume of V(x)/Al catalysts decrease progressively with increasing V loading. This phenomenon can be attributed, in part, to the inherently low surface area of VOx, where its contribution to the overall surface area becomes more significant as the V content increases [14,15,19]. Additionally, the clogging of the γ-Al_2O_3 pores by VO_x species may contribute to this reduction. It's worth noting that even when accounting for the presence of V_2O_5 and removing the contribution of VO_x (by considering it proportional to the V content) from the BET surface area, the resulting value does not

match that of the bare support (e.g., 170 m^2 g^{-1} for V(11)/Al instead of 180 m^2 g^{-1} for lone γ-Al_2O_3). The pore diameter was obtained from the adsorption branch and the values for all catalysts are similar to the support.

Figure 1 shows the diffraction patterns of both the γ-Al_2O_3 support and the supported vanadium oxide catalysts. For catalysts with V loadings up to 6 wt%, the diffraction patterns closely resemble those of the support, with no discernible reflection associated with any other phase than γ-Al_2O_3. This observation suggests that in these catalysts, vanadium species are well-dispersed on the alumina support. However, for catalysts containing V loadings of 9 and 11 wt%, distinct and sharp V_2O_5 reflections become evident (15.3°, 20.2°, 21.7°, 26.1°, 31.0°, 34.2°, 51.3° and 72.5°) [20,21].

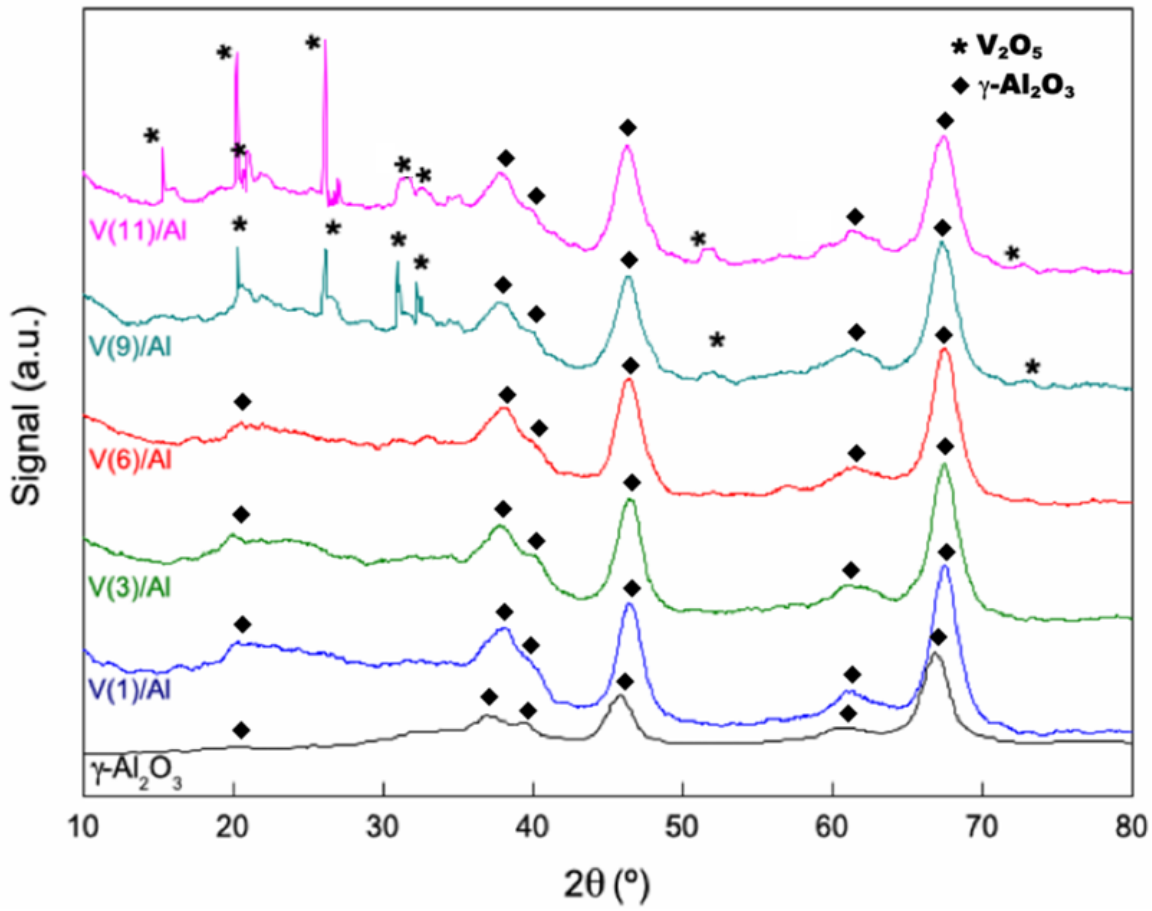

Figure 1: XRD pattern of V(x)/Al catalysts after calcination.

The Raman spectroscopy is a technique that is versatile and powerful for vanadium oxide characterization. The Raman spectra of the series of catalyst given on Figure 2 indicate that the V(9)/Al and V(11)/Al samples show the characteristic vibration bands of the bridging of V-O-V bonds of the V_2O_5 structure (102, 145, 196, 284, 305, 405, 480, 528, 701 and 993 cm^{-1}) [22,23]. On the spectrum of the V(6)/Al sample, some vibration bands of the V_2O_5 structure (the most intense) at 144 and 993 cm^{-1} are also visible. On this sample, Raman vibration bands are also observed at 245, 319, 594 and 944 cm^{-1} that would correspond to metavanadate $(VO_3)_n$ 2D species, according to the literature [24,25]. An additional band is slightly visible around 828 cm^{-1} that may be attributed to $[VO_4]^{3-}$ species, while another one at 180 cm^{-1} cannot be assigned.

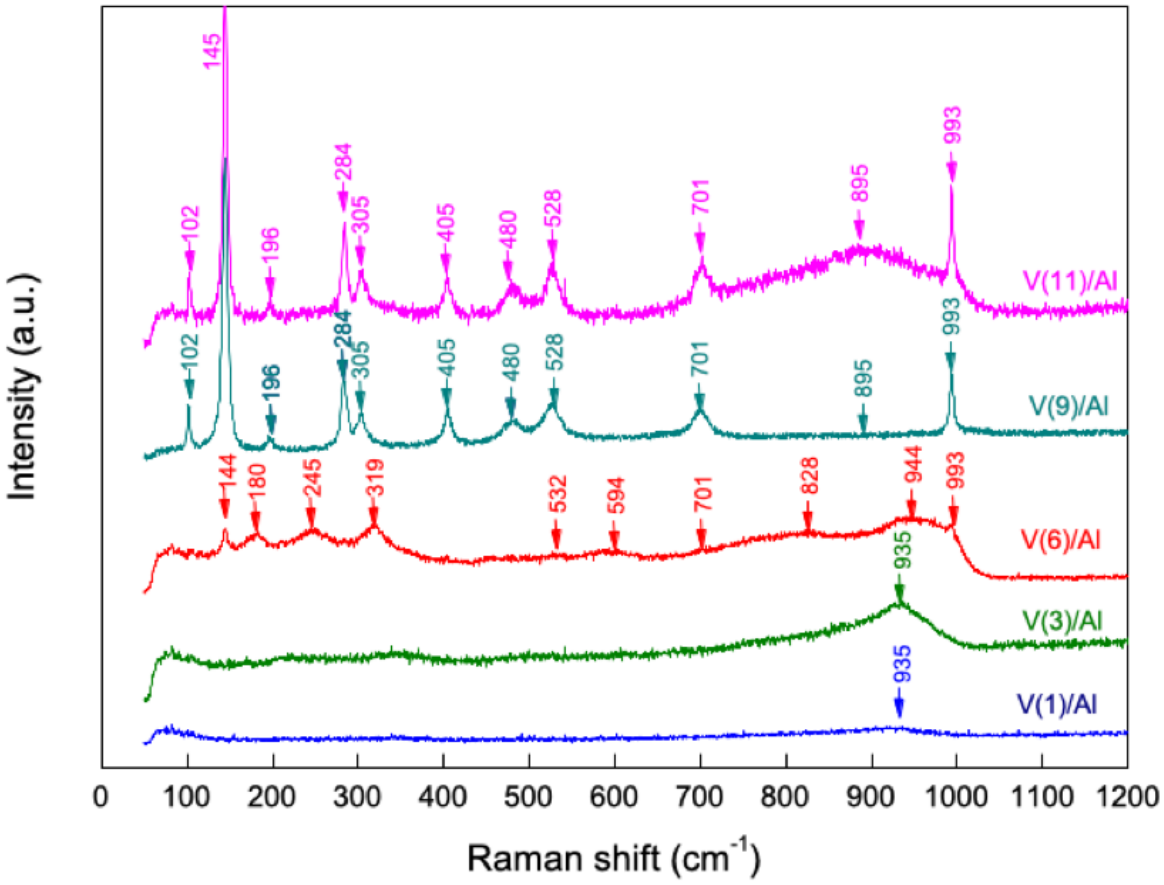

Figure 2: Raman spectra of V(x)/Al catalysts after calcination.

On the Raman spectra of the V(1)/Al and V(3)/Al samples, only a low intensity band is observed at 935 cm^{-1}, attributed to the presence of V-O-Al bonds [23], which could correspond to well-dispersed vanadium species, in line with the XRD results. For these two samples, the vibration bands corresponding to the V_2O_5 or $(VO_3)_n$ structures are not visible. These spectra are different from those obtained by Al-Ghamdi and de Lasa when varying the V content from 5 to 10 wt.% on the alumina support. They observed V_2O_5 species only for the highest loading of 10%, due to a better dispersion of vanadium species at the support surface [26]. This difference could be due to the different preparation method, which was performed in their case in the presence of oxalic acid at pH 2 that may favour the dispersion.

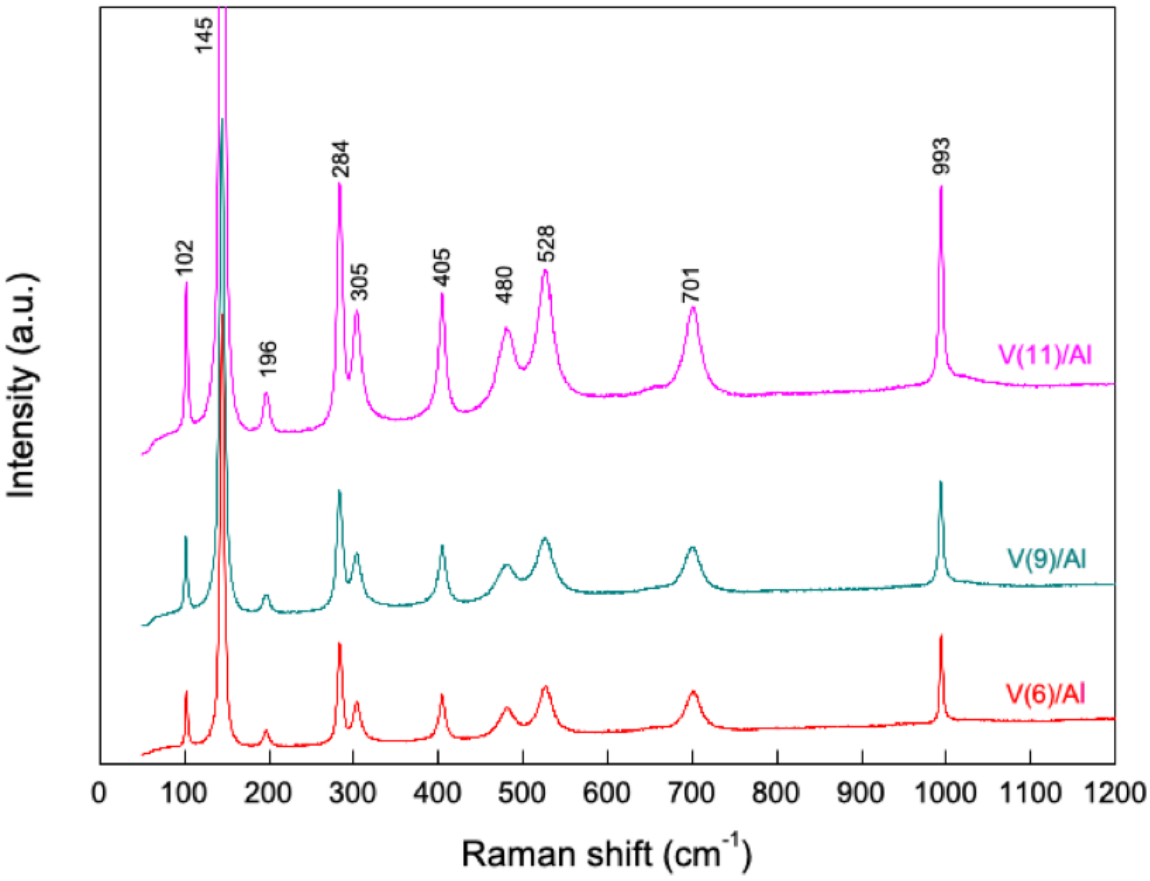

Figure 3: Raman spectra of micrometric particles visible under an optical microscope on V(6)/Al, V(9)/Al, V(11)/Al catalysts after calcination.

Under an optical microscope (100x magnification), used for micro-Raman spectroscopy, the V(6)/Al, V(9)/Al and V(11)/Al are in the form of micrometric particles, with various shapes and sizes. These micrometric particles, which take the form of platelets, are not visible on the V(1)/Al and V(3)/Al samples. The micro-Raman analysis of the microparticles allowed identifying only vibration bands corresponding to the V_2O_5 structure (Figure 3). For V(9)/Al and V(11)/Al depending on the microparticles analyzed, only the intensity of the bands varied, always corresponding to V_2O_5 species. For the V(6)/Al sample, Raman spectra registered in other parts are different from that presented in Figure 3, and similar to that presented in Figure 2, with peaks attributed to the V_2O_5 structure and others to metavanadate $(VO_3)_n$ species. In conclusion, it can be inferred that the number of V_2O_5 vanadium-rich platelets increases with the increase in vanadium content.

Samples with the lowest and highest vanadium content on the support (V(1)/Al and V(11)/Al) and a catalyst with intermediate loading (V(6)/Al) were also characterized by SEM. On the V(1)/Al catalyst, elemental analyzes were carried out in five different surface points, evidencing quite homogeneous mass concentrations, giving an average of about 53% for oxygen, 46% for aluminum and 1% for vanadium (the latter concentration varying between 0.54 and 1.20%), which correspond to a molar ratio between vanadium and aluminum, V/Al, of 0.011, similar to the actual ratio measured by ICP (c.a. 0.012). It can be seen in Figure 4(a) that, according to the elemental images, the vanadium distribution is homogeneous over the whole catalyst surface for V(1)/Al catalyst.

The same analysis was carried out on the V(11)/Al catalyst on eight different surface points, evidencing average mass concentrations of 39.4% for oxygen, 33.4% for aluminum and 27.2% for vanadium, with a molar ratio V/Al of 0.43, much higher than the one determined from ICP (around 0.116), due to the fact that probably multilayers or crystallites of vanadium oxide are deposited at the surface of the alumina support. It should be noted that

unlike the V(1)/Al catalyst, here the vanadium concentrations at the points analyzed varied significantly, from 3.5% to 71.5%. It can be seen in the elemental image (Figure 4(b)) that there are clearly places where vanadium is more concentrated and other places where its presence is practically null.

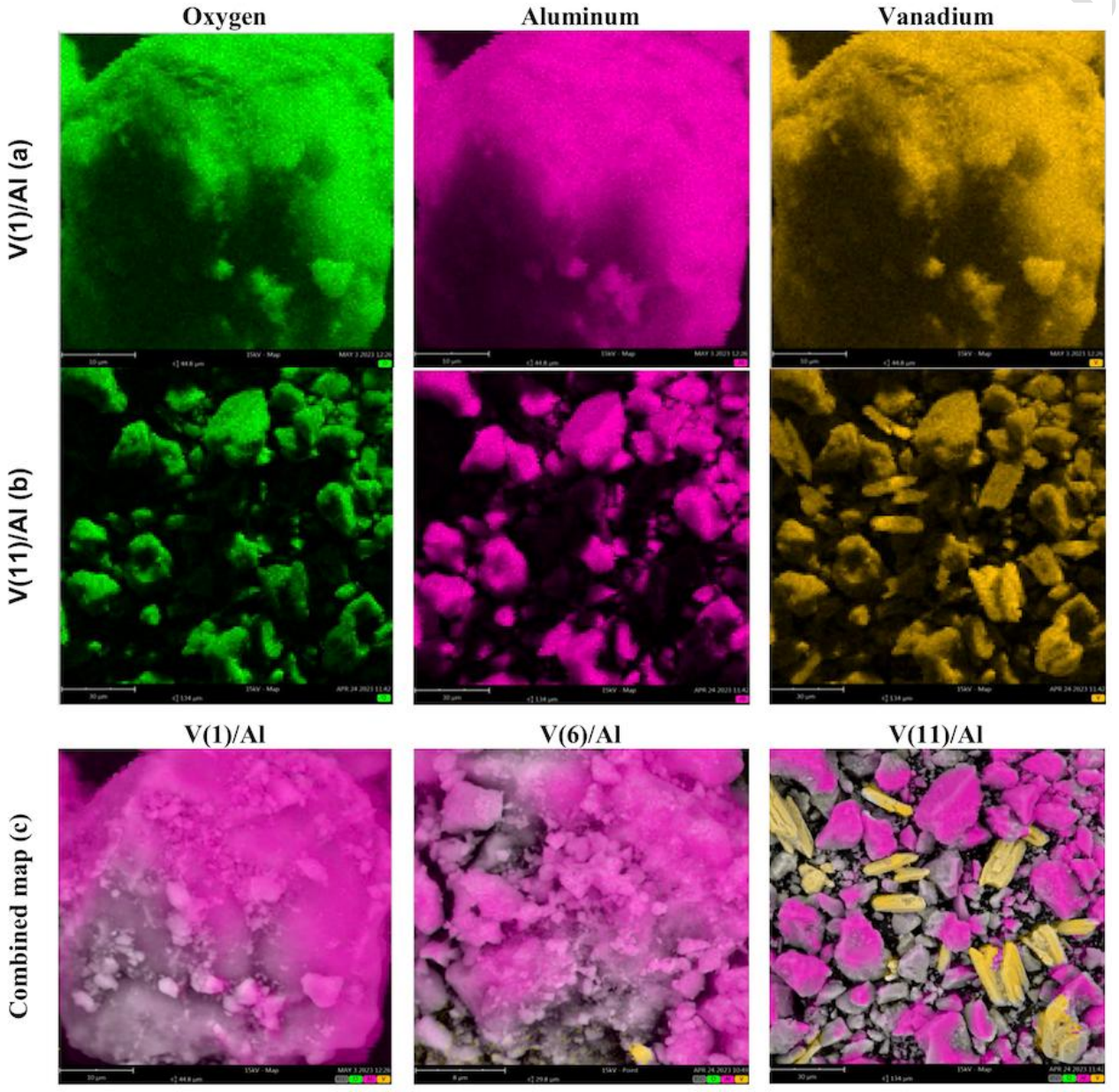

Figure 4: Analysis by SEM: (a) Elemental map of O, Al and V on the catalyst surface of the V(1)/Al sample. (b) Elemental map of O, Al and V on the surface of the V(11)/Al catalyst. (c) Combined elementary map of O, Al and V for V(1)/Al, V(6)/Al and V(11)/Al catalysts.

As an example, Figure 4(c) compares the combined element maps for the three catalysts V(1)/Al, V(6)/Al and V(11)/Al. For all samples, the signal of aluminum (in pink) is considerably stronger, covering systematically the signal of oxygen and vanadium. In the V(1)/Al catalyst, distinguishing the signal of vanadium from the background is difficult because of its low concentration. In the case of the V(6)/Al catalyst, the aluminum signal is still the most visible but the color is lighter than in the V(1)/Al sample, which may be due to the presence of more vanadium in these areas. In addition, a small vanadium-rich crystallite is clearly identified in Figure 4(c), which probably corresponds to the V_2O_5 platelets identified by micro-Raman. The distribution of the elements is less homogeneous compared to that of V(1)/Al, the mass concentrations being in this case: oxygen 54.8%, aluminum 41.9 % and vanadium 3.3%, lower than the one determined by ICP (5.4%) (V/Al molar ratio = 0.042 compared to c.a. 0.057 determined by ICP). This difference could be explained by the presence of a few vanadium-rich particles leading to a certain degree of heterogeneity.

In V(11)/Al catalyst, a large number of vanadium-rich particles is seen, that may correspond to V_2O_5 crystals according to Raman and XRD analyses. These vanadium species seem to be not in interaction with alumina, facilitating their clear identification.

Figure 5 shows the total acidity determined by TPD of pyridine and the strength distribution of acid sites, classified according to the desorption temperature into: weak ($T < 300$ °C), moderate ($300 < T < 500$ °C) and strong ($T > 500$ °C) [27].

The acidity of vanadium catalysts arises from two sources: the exposed alumina surface and the formation of a vanadate compound layer on the support material [28]. Two types of acid sites may also be present: Lewis acid sites (LAS), the only sites probed by pyridine adsorption on the bare alumina support, and Bronsted acid sites (BAS). VO_x species provide both types of acidity, with LAS and BAS, and consequently the addition of VO_x species will increase the acidity [24-26].

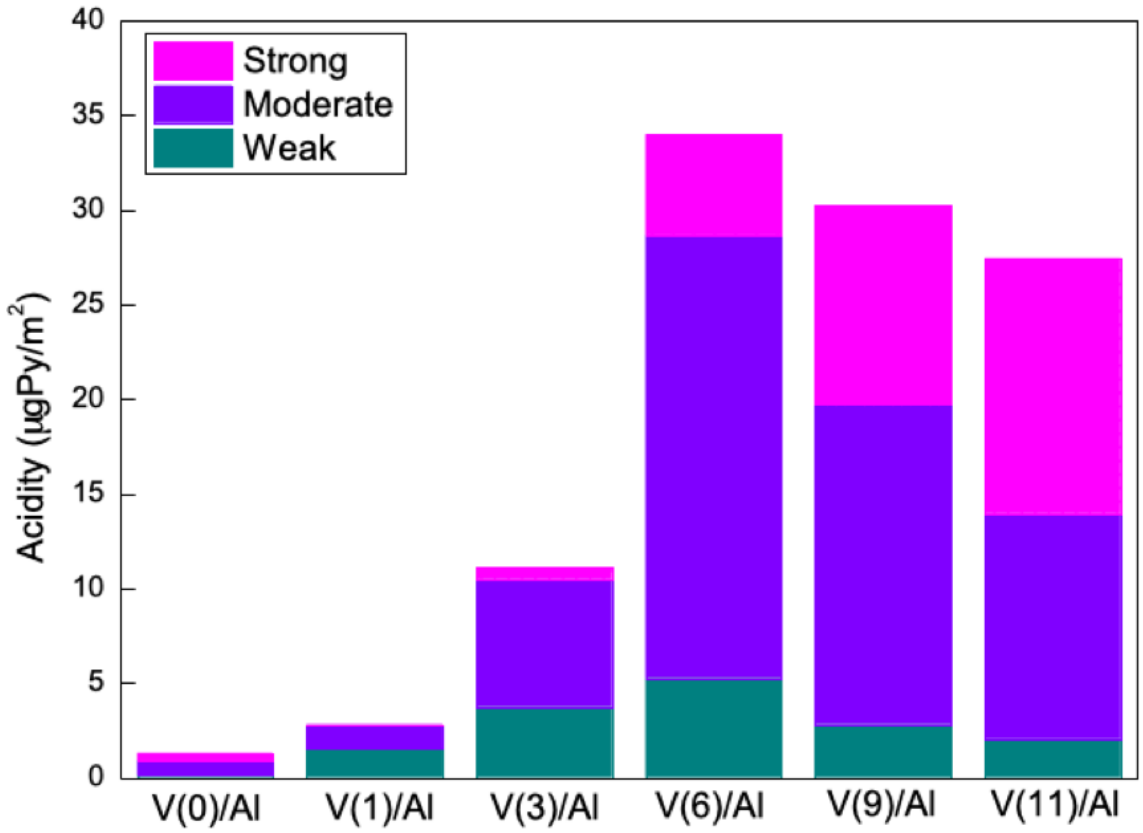

Figure 5: Total acidity and strength distribution of acidic sites (weak, moderate and strong) of the V(x)/Al catalysts determined by TPD-Py.

In the V loading range of 0–6 wt%, there is a noticeable increase in the total acidity as the concentration of VO_X species rises (as shown in Figure 5). This trend aligns with findings reported in the literature [24-26]. However, at higher V loadings (specifically 9 and 11 wt% V), there is a decrease in total acidity, these two catalysts being less acidic than the V(6)/Al sample. This decrease in total acidity can likely be attributed to the formation of bulk V_2O_5, which is known to exhibit lower acidity compared to the VO_X vanadate species [27, 28]. By the other hand, with an increase in vanadium loading, there is a shift in the distribution of acid sites. This results in a reduction in the proportion of weak acid sites. Conversely, a greater abundance of strong acid sites becomes evident at higher vanadium loadings.

V(6)/Al is the catalyst with the highest proportion of moderate acid site. It should be mentioned that BAS, due to hydroxylated VO_X species, would probably disappear after the pretreatments [23], especially those at high temperature performed before the catalytic test. The oxidation state of the surface VO_X species of the catalysts was assessed by XPS spectroscopy. The results are shown in Figure 6 for V(3)/Al, V(6)/Al, V(9)/Al and V(11)/Al catalysts. V(1)/Al is not shown because the V $2p_{3/2}$ signal intensity was too low.

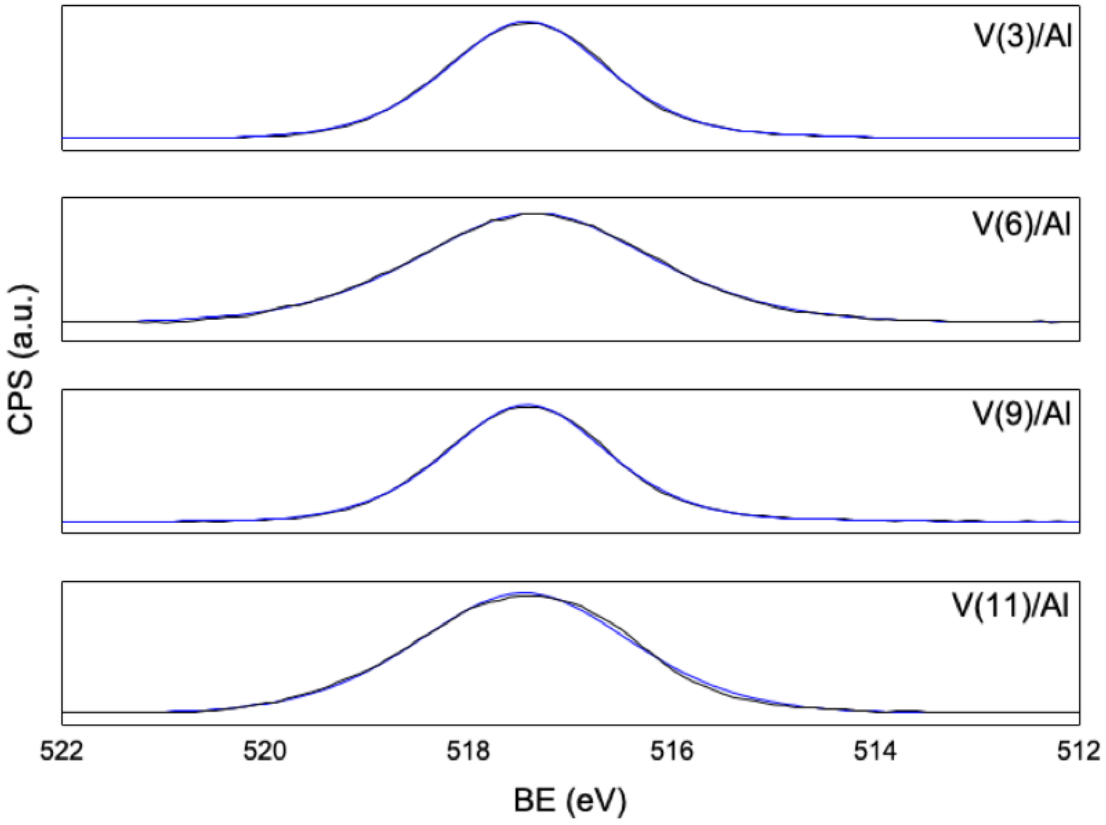

Figure 6: V $2p_{3/2}$ signal of V(3)/Al, V(6)/Al, V(9)/Al and V(11)/Al catalysts obtained by XPS spectroscopy.

Deconvolution of the V $2p_{3/2}$ peak revealed a single peak at binding energy between 517.40 and 517.45 eV, which is slightly lower than the reference value for V_2O_5 at 517.89 eV, as characterized under the same conditions. It can therefore be inferred that only V^{5+} species

are present on the surface, regardless the vanadium loading. This is consistent with the results of the other characterization techniques, which is expected since the catalysts were calcined after impregnation synthesis. This is also in accordance with the results of Shan et al. [29] demonstrating that after calcination all the vanadium species were in the form of V^{5+}, V^{4+} entities being absent in all their VO_X/Al_2O_3 catalysts.

Results of XPS analysis, notably the obtained V/Al molar ratio compared with the V/Al ratio determined by ICP, are gathered for all catalysts in Table 2.

Table 2: XPS analysis of V(x)/Al catalysts, with V/Al molar ratios determined by XPS and ICP.

Catalysts	B.E $V2p_{3/2}$, eV	FWHM[a]	V/Al, mol/mol	V/Al, mol/mol (ICP)
V(1)/Al	n.d.	n.d.	n.d.	0.012
V(3)/Al	517.51	2.6	0.036	0.031
V(6)/Al	517.36	2.7	0.046	0.057
V(9)/Al	517.44	1.9	0.068	0.096
V(11)/Al	517.17	2.4	0.107	0.116

[a] FWHM: Full width at half maximum

Except for V(3)/Al, the V/Al ratios determined by XPS are slightly lower than the values obtained by ICP. This variation is clearly related to the distribution of vanadium species with differing structures and crystallite sizes on the catalyst surface.

The reducibility of vanadium species is thought to influence catalytic performance, given that the ODH reaction follows a Mars-van-Krevelen redox cycle [16]. Therefore, the reducibility of the supported VO_X species was investigated through TPR experiments. The TPR profiles are shown in Figure 7 and the results are summarized in Table 3.

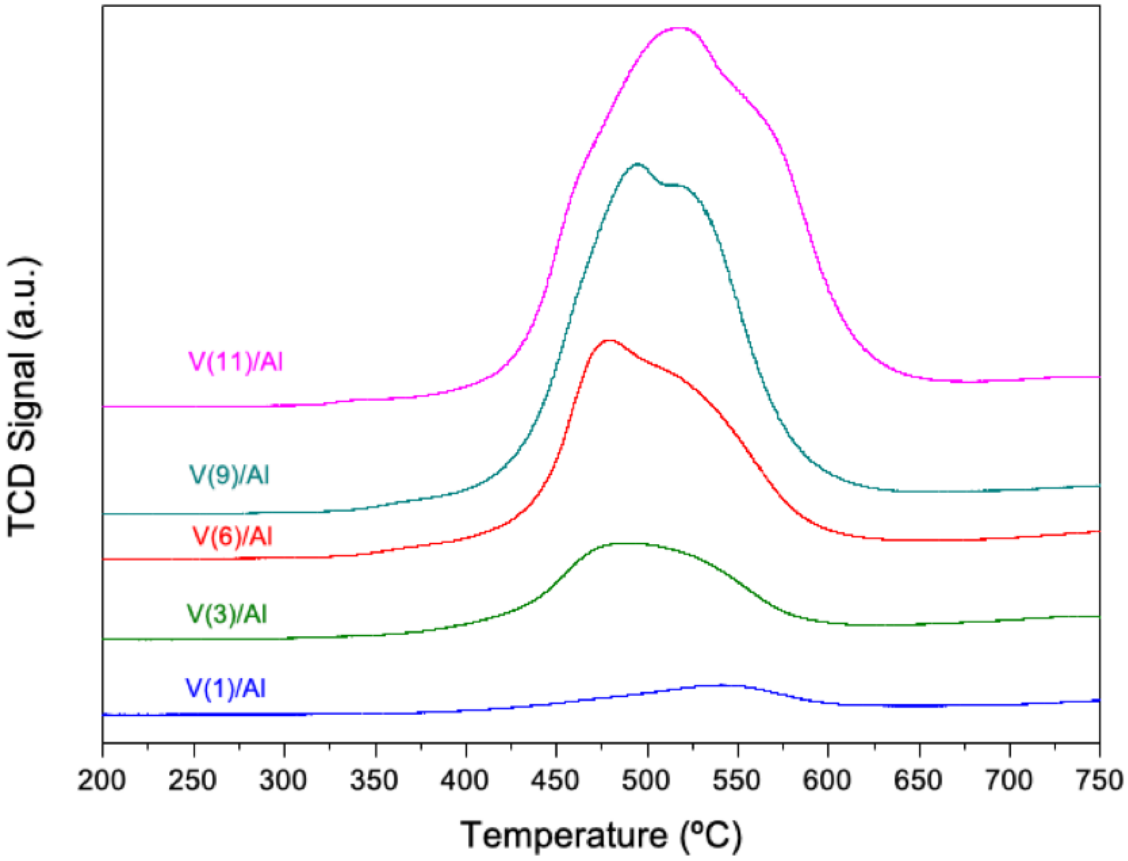

Figure 7: Temperature programmed reduction profile of the V(x)/Al catalysts.

As shown in Figure 7, the TPR profiles for the V(x)/Al catalysts demonstrate a dependence between the reduction behavior of the vanadium species and the vanadium loading. There is a clear increase in both the amount of H_2 consumed and the reduction temperature as the vanadium content in the catalyst increases. H_2/V ratios of 0.45, 0.60, 0.75, 0.75 and 0.80 were obtained for the V(1)/Al, V(3)/Al, V(6)/Al, V(9)/Al and V(11)/Al catalysts, respectively. These results indicate a direct relationship between surface VO_X density and reducibility. Higher reducibility was observed for catalysts with higher VO_X densities.

The V(1)/Al and V(3)/Al catalysts exhibit a single reduction peak centered at 550 °C and 480 °C, respectively, which can be attributed to the reduction of highly dispersed V^{5+} oxide species [30]. Notably, this reduction peak occurs at a higher temperature for V(1)/Al

compared to V(3)/Al and V(6)/Al catalysts. Based on the results of previous studies, this higher reduction temperature is attributed to the presence of ultra-highly dispersed vanadium oxide species on the surface of V(1)/Al catalyst [21, 31], with a strong interaction between V^{5+} and the γ-Al_2O_3 support.

Table 3: TPR results of V(x)/Al catalysts.

Catalyst	T_{red}, ºC	T_{M1}, °C	T_{M2}, °C	H_2/V	AOS
V(1)/Al	400	550	-	0.45	4.1
V(3)/Al	425	480	-	0.60	3.8
V(6)/Al	420	475	525	0.75	3.5
V(9)/Al	425	500	525	0.75	3.5
V(11)/Al	430	525	560	0.80	3.4

T_{red} = Temperature where the reduction starts, T_{Mi} (i = 1 or 2 for first and second peak, respectively) = Temperature at the maximum reduction; H_2 consumption expressed as H_2/V molar ratio; average oxidation state (AOS) after reduction calculated from the H_2 consumption (H_2/V molar ratio): AOS = 5-x with x = 2 H_2/V considering the following reduction reaction $V^{5+} + x/2\ H_2 \rightarrow V^{(5-x)+} + x\ H^+$.

On the basis of the H_2/V values presented in Table 3, it is evident that in the case of V(1)/Al, there is a minimal proportion of reducible VO_X species. For this catalyst, the average oxidation state calculated from the H_2/V value, starting from V^{5+}, is higher than 4.0, showing that for this sample the reduction of V^{5+} is not complete. The reduction of the other catalysts starts at higher temperatures, and the AOS value is lower than 4, indicating that the reduction of V^{5+} toward a lower oxidation state may be complete. For V(6)/Al, V(9)/Al and V(11)/Al, there are two reduction peaks: a first peak at T_{M1} between 475 and 525 °C and a second reduction peak T_{M2} appearing as a shoulder around 525-560 °C. Among all

the catalysts, except V(1)/Al, which is hardly reducible, the V(6)/Al sample begins to reduce at the lowest temperature, with T_{M1} being minimal. Furthermore, Table 3 shows that the H_2/V ratio values for the V(6)/Al, V(9)/Al and V(11)/Al catalysts are higher than those for the V(1)/Al and V(3)/Al catalysts. This suggests a direct correlation between surface VO_X density and reducibility. Catalysts with greater VO_X densities show a higher degree of reducibility, as evidenced by the decrease in average oxidation state (AOS) value with increasing the vanadium loading. This indicates that polymeric or crystalline vanadium species may undergo more extensive reduction compared to isolated vanadium species [32].

3.2. Catalytic performance

An extensive investigation was conducted on the oxidative dehydrogenation of propane reaction using V(x)/Al catalysts which were precalcined in air at 500 °C for 4 h as described in the catalyst preparation section. Various parameters such as reaction temperature, vanadium loading on the alumina support, and propane/oxygen ratio in the feed were studied. During the whole reaction time (240 min), the main products identified were propylene, CO, CO_2, and H_2O. The oxidative dehydrogenation reaction progressed sequentially, forming CO_X species through consecutive oxidations of propylene. Additionally, minor amounts of ethylene, ethane, and methane were observed, named further as cracking products.

3.2.1. Effect of reaction temperature and vanadium loading on the catalytic activity

The turn-over frequency (TOF) is a measure of specific activity, calculated as the moles of propane converted per mole of vanadium (based on the XPS results) and per unit of time using Equation (1).

Table 4 presents the TOF results obtained during the ODH reaction for V(x)/Al catalysts with varying amounts of vanadium (1, 3, 6, 9 and 11 wt% of V) within the temperature range of 300 < T(°C) < 550. Each experiment used a new catalyst, and the total reaction time was 240 minutes at each temperature.

Table 4: Turn-over frequency (TOF) ($x10^3$ s^{-1}) at 10 min reaction time. Reaction conditions: catalyst mass = 100 mg, propane flow rate = 15 cm^3 min^{-1}, C_3/O_2 ratio = 2.5.

Temperature, ºC	V(1)/Al	V(3)/Al	V(6)/Al	V(9)/Al	V(11)/Al
300	0.76	0.25	0.33	0.22	0.15
350	3.05	1.34	2.05	1.88	1.20
450	5.54	2.90	3.99	3.90	2.52
550	8.10	3.32	4.08	3.99	2.51

As shown in Table 4, both temperature and vanadium content have a significant effect on the TOF values. While the TOF increases with temperature whatever the catalyst, the V(1)/Al sample is the most active catalyst whatever the temperature. Except for the reaction temperature of 300 °C for which the TOF values for V(3)/Al and V(9)/Al can be considered as similar, for higher temperatures, the TOF values decrease in the following ranking: V(1)>V(6)>V(9)>V(3)>V(11), the catalyst with the highest V loading being the less active. This phenomenon is probably due to the agglomeration of V species and the formation of polymerized species (V_2O_5), as evidenced by XRD and Raman analyses (Figures 1 and 2). It was demonstrated by TPR that the reducibility increases with the V loading, but it does not lead to an increase in the activity, showing that the type of VO_X species probably plays a determining role in catalytic performance, instead of the redox properties.

Figure 8 provides valuable insights into the variations in propylene selectivity at different reaction temperatures across all V(x)/Al catalysts.

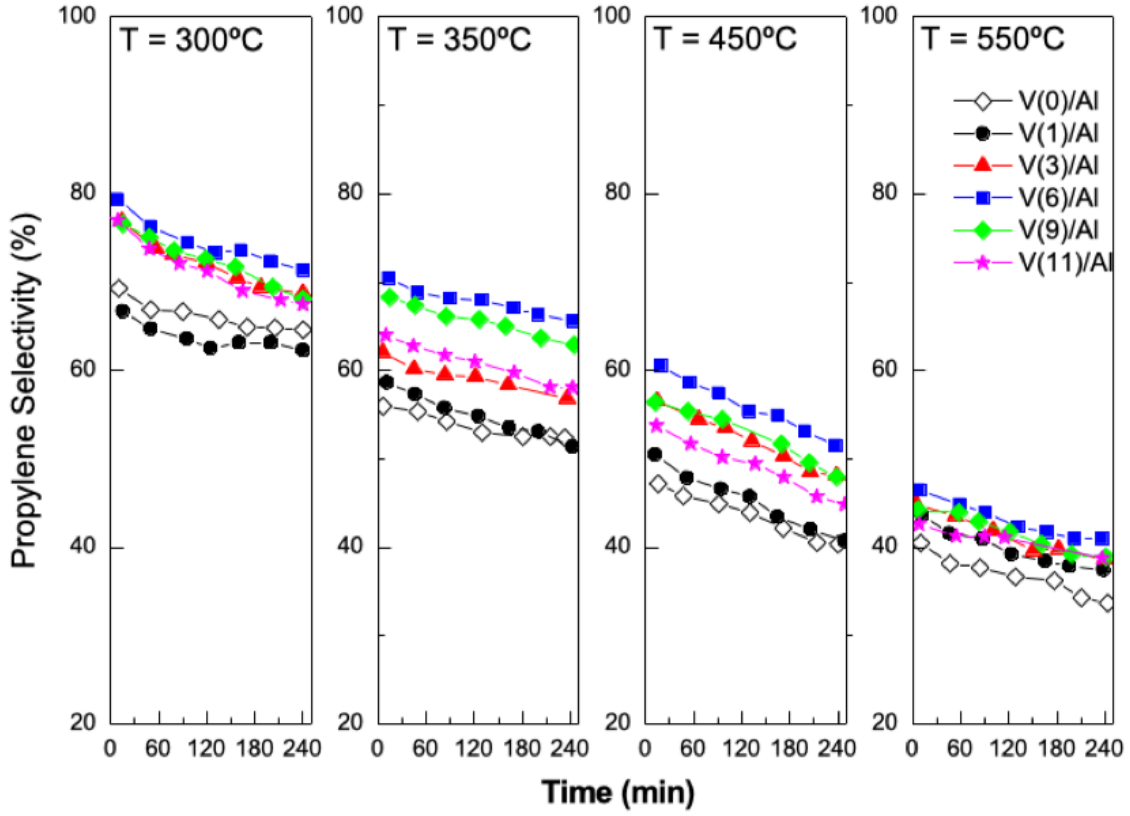

Figure 8: Selectivity to propylene as a function of reaction time for different temperatures for each V(x)/Al catalyst during ODHP reaction. Reaction conditions: catalyst mass = 100 mg, propane flow rate = 15 cm^3 min^{-1}, C_3/O_2 ratio = 2.5.

A clear trend emerges as propylene selectivity decreases with increasing reaction temperature, resulting in higher formation of carbon oxides and cracking products. Regarding propylene selectivity as a function of vanadium loading, a clear pattern is observed, with optimal selectivity achieved using the V(6)/Al catalyst.

Figure 9 shows the relationship between propylene selectivity and TOF at 10 min reaction time.

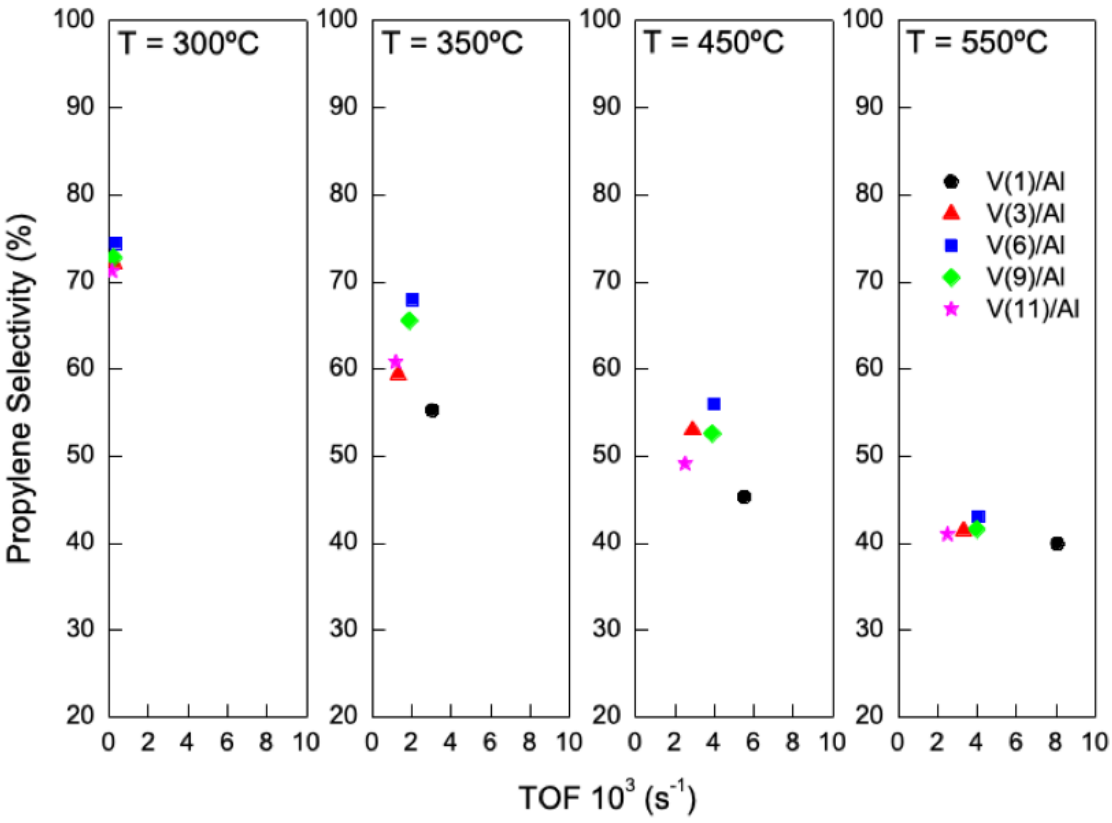

Figure 9: Selectivity to propylene as function of TOF at 10 min reaction time for different temperatures for each V(x)/Al catalyst during ODHP reaction. Reaction conditions: catalyst mass = 100 mg, propane flow rate = 15 cm^3 min^{-1}, C_3/O_2 ratio = 2.5.

The data highlight that the maximum propylene selectivity values are attained at 300 ºC, but at this low temperature, the TOF remains relatively low, about 0.7 s^{-1}. Significant propylene selectivity values are noted at 350 ºC, a relatively low temperature in an industrial setting. At this temperature, the optimum selectivity of 68% is attained for a vanadium loading of 6 wt%, leading to a TOF = 2.05 s^{-1} at 10 min reaction time.

Therefore, the best performance in the ODH reaction is determined not only by the amount of active sites in the catalysts, but also by the type of VO_X species. Y. Gambo et al. [33] emphasized the critical role of the active sites of the catalyst in the catalytic stabilization of intermediates and the direction of the reaction toward the desired product.

The selectivities for various products during the ODHP reaction at 350 °C (considered as the most optimal temperature, Figure 9) are depicted in Figure 10 for each V(x)/Al sample.

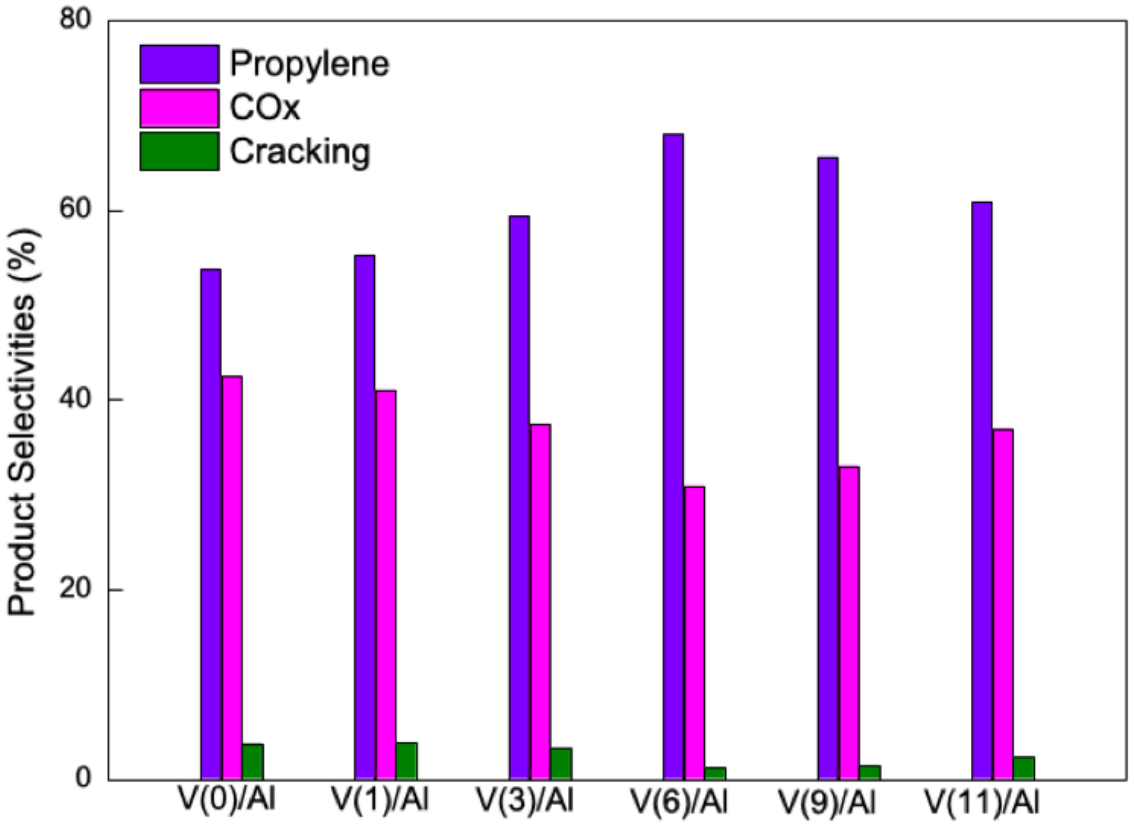

Figure 10: Selectivities to propylene, CO_X and cracking products during the ODHP after 240 min reaction time. Reaction conditions: catalyst mass = 100 mg, T = 350 ºC, propane flow rate = 15 cm^3 min^{-1}, C_3/O_2 ratio = 2.5, time on stream = 240 min.

It can be seen that the V(0)/Al sample, that does not contain vanadium, is the catalyst that presents the lowest selectivity to propylene, due to the highest selectivity to CO_x, the main by-product, and cracking products. Consequently, the alumina support favors the formation of undesired products. It has been proposed that the differences in selectivity to dehydrogenation reactions could be controlled, apart from the acid–base character [34, 35], by the type of V species and the distance between the active sites [24]. When V is added

on the alumina support, the selectivity to propylene increases up to 6 wt.% of V, the V(6)/Al catalyst exhibits then a minimum selectivity for CO_X and cracking products. This property is attributed to the presence in this catalyst of monomeric and polymeric VO_x entities [24, 34, 36], along with a limited amount of V_2O_5 crystalline species. The increase of the coverage of alumina by vanadium species may decrease the support role in the formation of CO_x and cracking products when VO_x species are well-dispersed or low-polymerized to cover the alumina. For the catalysts with high vanadium loadings (V(9) and V(11)/Al samples), the lower propylene selectivity is due to the increase of the amount of crystalline 3D V_2O_5 species on the surface, not in interaction with alumina, as seen on the SEM images, liberating the accessibility to the alumina support.

3.2.2 Deactivation process

As observed in the results presented previously, during the 240 min reaction time, the selectivity towards propylene decreases. An investigation was conducted to identify the source of this deactivation using experimental techniques such as temperature programmed oxidation (TPO). Coke formation was observed even in the presence of molecular oxygen in the reaction medium, because the reaction temperature used for ODHP was lower than that needed to burn all the coke, that is, greater than 600 ºC [37].

The TPO results presented in the Figure 11(A) show an increase in coke deposition with both the reaction temperature and the vanadium loading on the catalyst. This suggests that there is a deposition of carbon on the surface of the VO_X sites, effectively covering them, preventing propane adsorption and, consequently, contributing to the deactivation of the catalyst. The experimental results emphasize the significant influence of the VO_X species structure, especially the charge of V, on coke formation. No direct correlation was observed between total catalyst acidity and carbon deposition, however, the characterization results

showed that the structure of the vanadium species in the catalyst influenced its acidity. As the surface density of vanadium and the size of the VO_X species increase, the probability of interactions between different adsorbed propylene molecules also increases, resulting in higher carbon deposition [38].

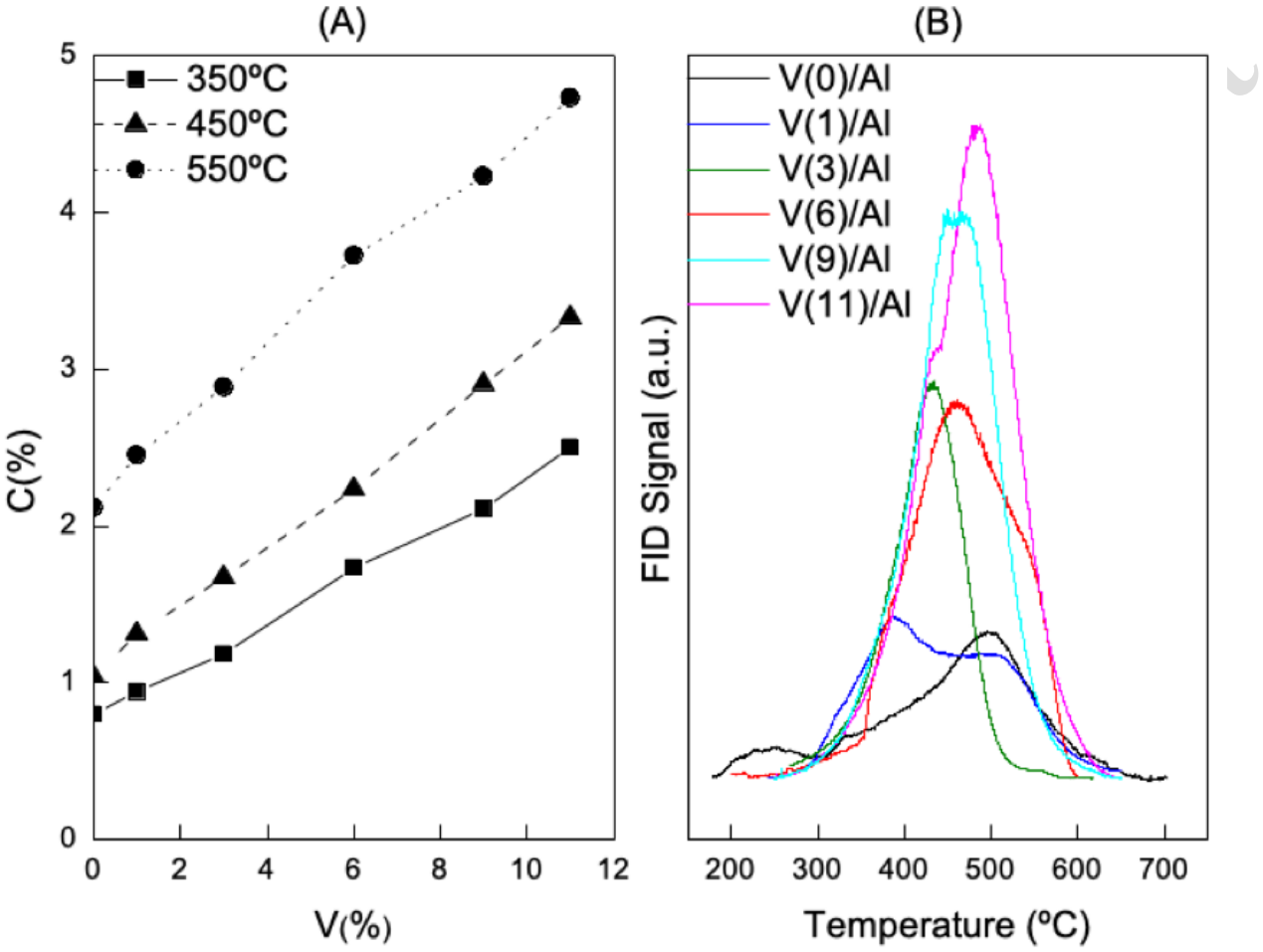

Figure 11: (A) Coke deposited (wt%) as a function of vanadium loading (wt%) obtained at different ODHP reaction temperatures after 240 min reaction time (propane flow rate = 15 cm^3 min^{-1}, C_3/O_2 ratio = 2.5). (B) TPO profiles post ODHP reaction at 350 ºC.

Figure 11(B) shows the TPO profiles where it can be seen that there is a variation in the maximum coke combustion temperature, probably due to the presence of different coke species [39]. The profile of the V(0)/Al catalyst shows a peak at a maximum temperature of about 500 ºC. In contrast, the V(1)/Al catalyst's profile exhibits a first peak at a lower

temperature of about 400 ºC. As the vanadium content increases, a single massif, which can be decomposed into two peaks, is observed at a maximum temperature centered between 420-500 ºC. The literature emphasizes that coke deposited near the VO_X sites undergoes easier oxidation compared to coke deposited on the support [29, 40]. On the other hand, in Figure 11(B) it can be observed that as the vanadium content rises, there is a significant increase in the peak intensity centered at higher temperatures. This phenomenon could be attributed to the migration of carbonaceous species from the VO_X sites towards the support.

To better characterize the species present on the catalyst surface, two samples, V(1)/Al and V(11)/Al, were analyzed after catalytic test with C_3/O_2 ratio of 2.5 at 350°C. For the V(1)/Al sample, only bands characteristics of carbon were clearly observed in some isolated areas. In the other parts, the Raman signal was masked due to strong luminescence, likely caused by the presence of organic species provided by reactant and products on the sample surface. On the V(11)/Al sample, some microparticles corresponding to V_2O_5, similar to those observed on the fresh sample but in lower amounts, were detected. In other parts of the same sample, two types of Raman spectra were observed, one corresponding to pure carbon, and another one indicating the presence of both carbon and hydrated V_2O_5 species, likely resulting from water formation along with COx species during the propane ODH reaction.

3.2.3. Effect of the C_3/O_2 ratio

To optimize propylene selectivity, it is critical to minimize reactions that lead to the formation of carbon oxide compounds, a process often facilitated by the presence of oxygen in the reaction environment. With this in mind, an investigation was conducted to evaluate the effect of varying propane-to-oxygen ratios on the performance of the V(6)/Al

catalyst, previously identified as exhibiting the most favorable behavior in ODHP. Various propane-to-oxygen ratios (1.6, 2.5 and 3.3) in the reactor feed were studied.

Figure 12 shows the evolution of conversion and selectivity to propylene and CO_X over time with different propane-to-oxygen ratios, and gives the values of coke deposited as wt% C after 240 min reaction time.

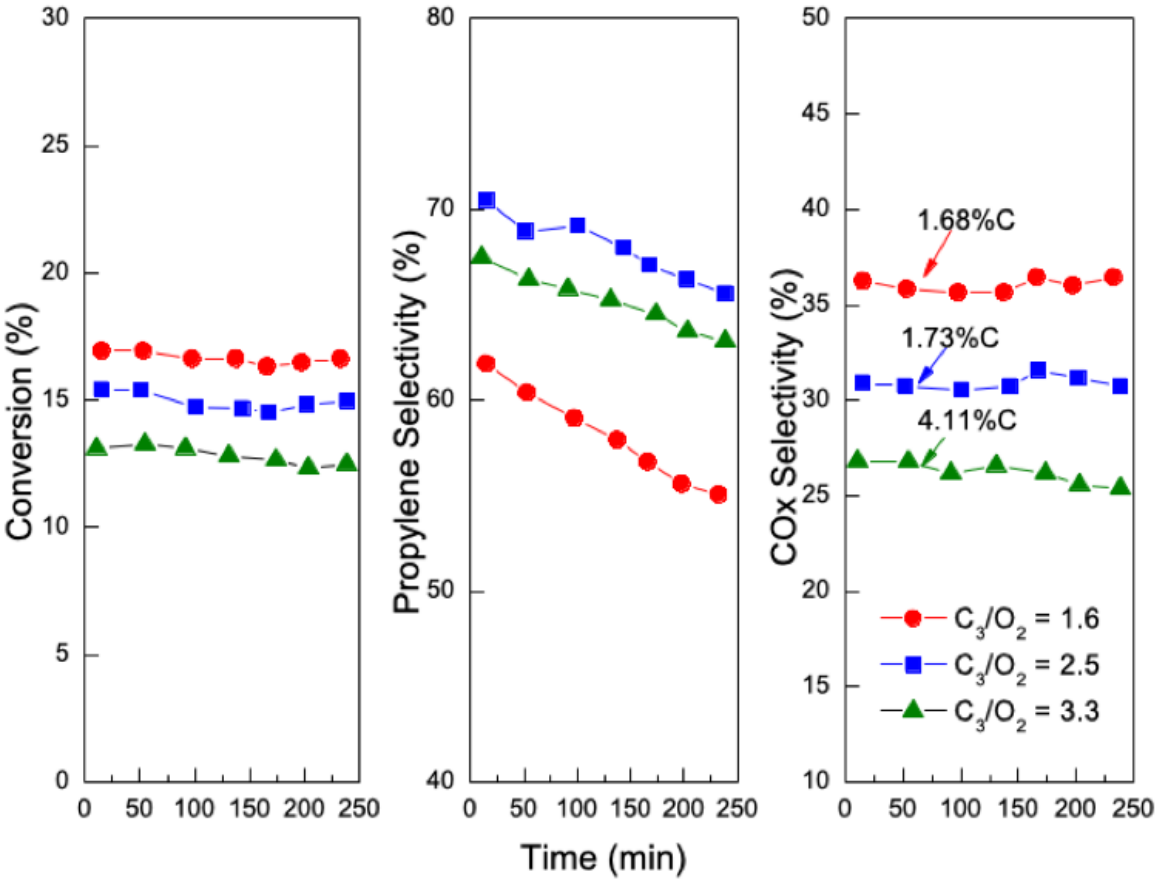

Figure 12: Effect of propane-to-oxygen molar ratio on the performances of the V(6)/Al catalyst obtained during ODHP: Conversion (%), Selectivity to propylene (%) and Selectivity to CO_x (%) as a function time (together with the value of coke deposited at the end of the reaction, wt%C). Reaction conditions: catalyst mass = 100 mg, T = 350 °C, propane flow rate = 10, 15 and 20 cm^3 min^{-1}, C_3/O_2 ratio = 1.6, 2.5 and 3.3.

In particular, there is a noticeable decrease in propane conversion as the propane-to-oxygen ratio increases. At the same time, there is a maximum in selectivity toward propylene for the propane-to-oxygen ratio equal to 2.5. This result reflects two distinct trends: at higher C_3/O_2 ratios, where less oxygen is available in the reaction medium, propylene selectivity decreases at the expense of coke formation. Conversely, at lower ratios, propylene selectivity decreases primarily due to deep oxidation processes leading to the production of CO_X compounds and low coke deposition. The data clearly show that the most favorable catalyst behavior (high propylene selectivity with intermediate carbon formation) is achieved by maintaining a propane-to-oxygen ratio of 2.5.

4. Conclusions

The effect of vanadium loading on the properties of VO_x/Al_2O_3 catalysts was evaluated in a wide range of contents, from 1 to 11 wt.% for the oxidative dehydrogenation reaction. It was demonstrated that the most active V species were those that were well dispersed at the alumina surface, with a strong interaction of the support, leading to V-O-Al species. However, the alumina surface presents Lewis acid sites, which are detrimental to the selectivity to propylene, favoring the formation of undesirable products, mainly CO_x species. The increase of the V loading increases the acidity of the catalysts, with a positive effect on the selectivity due to the coverage of the acidic sites of the alumina support. Higher vanadium loadings induce also formation of polymerized vanadium species that were observed at V loadings higher than 6 wt.%. V_2O_5 crystallites, that are majority at high vanadium loading (V(9) and V(11)/Al catalysts) were clearly seen by SEM where they appeared as separated from the alumina support. As a result, the selectivity to propylene increases with the V content up to 6 wt.%, due to the coverage of alumina by V species, and then decreases a little due to the formation of the 3D large V_2O_5-rich crystallites. The

reducibility of the V^{5+} species, which is the most important for high V loading when V_2O_5 crystallites have been identified, seems to not play a key-role in the reaction, highly dispersed V^{5+} species in strong interaction with the support identified in majority on the V(x)/Al catalysts with low V contents being more accessible and more active for propane ODH. The elucidated structure-property relationship serves as a guide for the preparation of supported VO_X catalysts suitable for ODHP: well-dispersed V species must be favored up to high V contents by using appropriate preparation method to cover the alumina and avoid the formation of 3D V_2O_5 crystallites.

On the other hand, the reaction temperature and the C_3/O_2 ratio are two important experimental variables that influence the behavior of the catalysts in oxidative dehydrogenation of propane, which is related to the fact that the studied reaction occurs in successive stages.

It was observed that the deactivation of the catalysts is due to the accumulation of coke. According to the TPO results, it can be concluded that the amount of coke deposition is related to the vanadium loading on the catalyst and therefore to the degree of polymerization of the VO_X species. The higher the degree of polymerization of the VO_X species, the greater the deposition of coke on the catalyst surface. On the other hand, the presence of multiple peaks in the TPO profiles can be related to the different sites of coke deposit according to the V content of the catalysts. In addition, the variation in the maximum combustion temperature of coke is probably due to the presence of carbon of different nature, a property influenced by the different types of surface vanadium species present in each catalyst studied.

Acknowledgment

The authors thank the CONICET and CNRS for its financial support for collaboration between the INCAPE and IC2MP laboratories as part of the international research project OLECAT. The authors from IC2MP acknowledge financial support from the European Union (ERDF) and “Région Nouvelle Aquitaine” and indicate that this work pertains to the French government program "Investissements d'Avenir" (EUR INTREE, reference ANR-18-EURE-0010). The XPS services, and in particular Christine Canaff, are thanked for data characterization and analysis.

References

[1] M.L. Balogun, S. Adamu, I.A. Bakare, M.S. Ba-Shammakh, M.M. Hossain. CO_2 Assisted Oxidative Dehydrogenation of Propane to Propylene over Fluidizable MoO_3/La_2O_3-γAl_2O_3 *Catalysts J. CO_2 Util*. 2020, 42, 101329.

https://doi.org/10.1016/j.jcou.2020.101329

[2] Yang Wang, Wen-Cui Li, Yu-Xi Zhou, Rao Lu, An-Hui Lu. Boron nitride wash-coated cordierite monolithic catalyst showing high selectivity and productivity for oxidative dehydrogenation of propane. *Catal. Today* 2020, 339, 62-66.

https://doi.org/10.1016/j.cattod.2018.12.028

[3] Son Dong, Natalie R. Altvater, Lesli O. Mark, Ive Hermans. Assessment and comparison of ordered & non-ordered supported metal oxide catalysts for upgrading propane to propylene. *Appl. Catal. A: Gen.* 2021, 617, 118121.

https://doi.org/10.1016/j.apcata.2021.118121

[4] Cheng Zuo, Man Wu, Xiuli Zhang, Qingjie Guo. CeO_2-CrO_y/γ-Al_2O_3 redox catalyst for the oxidative dehydrogenation of propane to propylene. *Can. J. Chem. Eng.* 2021, 99, 235-250.

https://doi.org/10.1002/cjce.23824

[5] Harold H. Kung. Oxidative Dehydrogenation of Light (C_2 to C_4) Alkanes. *Adv. Catal.* 1994, 40, 1–38.

https://doi.org/10.1016/S0360-0564(08)60655-0

[6] Zeeshan Nawaz. Light alkane dehydrogenation to light olefin technologies: a comprehensive review. *Rev. Chem. Eng.* 31 (2015) 413–436.

https://doi.org/10.1515/revce-2015-0012

[7] Wayne Daniell, Anne Ponchel, Stefan Kuba, Franz Andrele, Thomas Weingand, Duncan Gregory, Helmut Knözinger. Characterization and Catalytic Behavior of VO_x-CeO_2 Catalysts for the Oxidative Dehydrogenation of Propane. *Top. Catal.* 2002, 30, 65–74.

https://doi.org/10.1023/A:1016399315511

[8] Yuvasri Ramesh, P Thirumala Bai, Haribabu Bathula, Lingaiah Nakka, Seetha Rama Rao Kamaraju, Potharaju S Sai Prasa. Oxidative dehydrogenation of ethane to ethylene on Cr_2O_3/Al_2O_3–ZrO_2 catalysts: the influence of oxidizing agent on ethylene selectivity. *Appl. Petrochem. Res.* 2014, 4 247-252.

https://doi.org/10.1007/s13203-014-0043-4

[9] Carlos A. Carrero, Robert Schloegl, Israel E. Wachs, Reinhard Schomaecker. Critical Literature Review of the Kinetics for the Oxidative Dehydrogenation of Propane over Well-Defined Supported Vanadium Oxide Catalysts. *ACS Catal*. 2014, 4, 3357-3380.

https://doi.org/10.1021/cs5003417

[10] Fabrizio Cavani, Nicola Ballarini, Antonio Cericola. Oxidative dehydrogenation of ethane and propane: How far from commercial implementation?. *Catal. Today* 2007, 127, 113-131.

https://doi.org/10.1016/j.cattod.2007.05.009

[11] Rick B. Watson, Umit S. Ozkan. K/Mo Catalysts Supported over Sol–Gel Silica–Titania Mixed Oxides in the Oxidative Dehydrogenation of Propane. *J. Catal.* 2000, 191, 12-29.

https://doi.org/10.1006/jcat.1999.2781

[12] Gheorghita Mitran, Rawaz Ahmed, Emmanuel Iro, Saeed Hajimirzaee, Simon Hodgson, Adriana Urda, Maria Olea, Ioan-Cezar Marcu. Propane oxidative dehydrogenation over VO_X/SBA-15 catalysts. *Catal. Today* 2018, 306, 260-267.

https://doi.org/10.1016/j.cattod.2016.12.014

[13] Fushan Feng, Haiyuan Zhang, Shaoqi Chu, Qinqin Zhang, Chao Wang, Guangjian Wang, Fang Wang, Liancheng Bing, Dezhi Han. Recent progress on the traditional and emerging catalysts for propane dehydrogenation. *J. Ind. Eng. Chem.* 2023, 118, 1–18.

https://doi.org/10.1016/j.jiec.2022.11.001

[14] Morris D. Argyle, Kaidong Chen, Alexis T. Bell, Enrique Iglesia. Effect of Catalyst Structure on Oxidative Dehydrogenation of Ethane and Propane on Alumina-Supported Vanadia. *J. Catal.* 2002, 208, 139-149.

https://doi.org/10.1006/jcat.2002.3570

[15] Uwe Rodemerck, Mariana Stoyanova, Evgenii V. Kondratenko, David Linke. Influence of the kind of VOx structures in VOx/MCM-41 on activity, selectivity and stability in dehydrogenation of propane and isobutane. *J. Catal.* 2017, 352, 256–263.

https://doi.org/10.1016/j.jcat.2017.05.022

[16] Soumik Chakraborty, Sudhir C. Nayak, Goutam Deo. TiO_2/SiO_2 supported vanadia catalysts for the ODH of propane. *Catal. Today* 2015, 254, 62-71.

https://doi.org/10.1016/j.cattod.2015.01.047

[17] Yuming Li, Xuezhi Yu, Qiyang Zhang, Vita A. Kondratenko, Yajun Wang, Guoqing Cui, Mingxia Zhou, Chunming Xu, Evgenii V. Kondratenko, Guiyuan Jiang. The nature of VO_X structures in HMS supported vanadium catalysts for non-oxidative propane dehydrogenation. *J. Catal.* 2022, 413, 658–667.

https://doi.org/10.1016/j.jcat.2022.07.017

[18] Viviana M. Benitez and Carlos L. Pieck. Influence of Indium Content on the Properties of Pt–Re/Al_2O_3 Naphtha Reforming Catalysts. *Catal Lett* 2010,136,45–51

https://doi.org/10.1007/s10562-009-0202-x

[19] Brishti Mitra, Israel E. Wachs, Goutam Deo. Promotion of the propane ODH reaction over supported V_2O_5/Al_2O_3 catalyst with secondary surface metal oxide additives. *J. Catal.* 2006, 240, 151–159.

https://doi.org/10.1016/j.jcat.2006.03.015

[20] Gang Liu, Zhi-Jian Zhao, Tengfang Wu, Liang Zeng, Jinlong Gong. Nature of the Active Sites of VO_x/Al_2O_3Catalysts for Propane Dehydrogenation. *ACS Catal.*2016, 6, 5207−5214.

https://doi.org/10.1021/acscatal.6b00893

[21] Frank Klose, Tania Wolff, Heike Lorenz, Andreas Seidel-Morgenstern, Yuri Suchorski, Monika Piórkowska, Helmut Weiss. Active species on γ-alumina-supported vanadia catalysts: Nature and reducibility. *J. Catal.* 2007, 247, 176–193.

https://doi.org/10.1016/j.jcat.2007.01.013

[22] Noelia Alonso-Fagúndez, Manuel López Granados, Rafael Mariscal, Manuel Ojeda. Selective Conversion of Furfural to Maleic Anhydride and Furan with VO_x/Al_2O_3 Catalysts. *ChemSusChem.* 2012, 6, 1984-1990.

https://doi.org/10.1002/cssc.201200167

[23] Zichun Wang, Yijiao Jiang, Wenjie Yang, Ang Li, Michael Hunger, Alfons Baiker , Jun Huang. Tailoring single site VO_4 on flame-made V/Al_2O_3 catalysts for selective oxidation of n-butane. *J. Catal.* 2022, 413, 93–105.

https://doi.org/10.1016/j.jcat.2022.06.013

[24] Chong Chen, Minglei Sun, Zhongpan Hu, Yuping Liu, Shoumin Zhang, Zhong-Yong Yuan. Nature of active phase of VO_x catalysts supported on SiBeta for direct dehydrogenation of propane to propylene. *Ch. J. Catal.* 2020, 41, 276–285.

https://doi.org/10.1016/S1872-2067(19)63444-3

[25] Mihaela Florea, Ricardo Prada Silvy, Paul Grange. Vanadium aluminium oxynitride catalysts for propane ammoxidation reaction: Effect of the V/Al ratio on the structure and catalytic behaviour**.** *Appl. Catal. A: Gen.* 2005, 286, 1–10.

https://doi.org/10.1016/j.apcata.2005.02.032

[26] Sameer A. Al-Ghamdi, Hugo I. de Lasa. Propylene production via propane oxidative dehydrogenation over VOx/γ-Al_2O_3 catalyst. *Fuel* 2014, 128, 120-140 https://doi.org/10.1016/j.fuel.2014.02.033

[27] Pei-Pei Li, Wan-Zhong Lang, Ke Xia, Luan Luan, Xi Yan, Ya-Jun Guo. The promotion effects of Ni on the properties of Cr/Al catalysts for propane dehydrogenation reaction. *Appl. Catal. A: Gen.*2016, 522, 172–179.

https://doi.org/10.1016/j.apcata.2016.05.007

[28] J. Le Bars, Jacques C. Vedrine, Aline Auroux, Sophia Trautmann, Manfred Baerns. Microcalorimetric and infrared studies of the acid base properties of V_2O_5 / γ-Al_2O_3 catalysts. *Appl. Catal. A: Gen.* 1994, 119, 341-354.

https://doi.org/10.1016/0926-860X(94)85201-4

[29] Yu-Ling Shan, Wen-Ting Zhao, Shi-Lei Zhao, Xiu-Xin Wang, Huai-Lu Sun, Wen-Long Yu, Jun-Wei Ding, Xiang Feng, De Chen. Effects of alumina phases on the structure and performance of VO_x/Al_2O_3 catalysts in non-oxidative propane dehydrogenation. *Mol. Catal.* 2021, 504, 111466.

https://doi.org/10.1016/j.mcat.2021.111466

[30] Qinglong Liu, Zhi Yang, Mingsheng Luo, Zhen Zhao, Jiayu Wang, Zean Xie, Lin Guo. Vanadium-containing dendritic mesoporous silica nanoparticles: Multifunctional catalysts for the oxidative and non-oxidative dehydrogenation of propane to propylene. *Micro. Meso. Mater.* 2019, 282, 133–145.

https://doi.org/10.1016/j.micromeso.2019.03.036

[31] Z. Wu, H-S. Kim, P. C. Stair, S. Rugmini, S. D. Jackson. On the Structure of Vanadium Oxide Supported on Aluminas: UV and Visible Raman Spectroscopy, UV−Visible Diffuse Reflectance Spectroscopy, and Temperature-Programmed Reduction Studies. *J. Phys. Chem. B* 2005, 109, 2793-2800.

https://doi.org/10.1021/jp046011m

[32] Roman Bulánek, Pavel Čičmanec, Hsu Sheng-Yang, Petr Knotek, Libor Čapek, ˇ Michal Setnička. Effect of preparation method on nature and distribution of vanadium species in vanadium-based hexagonal mesoporous silica catalysts: Impact on catalytic behavior in propane ODH. *Appl. Catal. A: Gen.* 2012, 415-416, 29-39.

https://doi.org/10.1016/j.apcata.2011.11.033

[33] Yahya Gambo, Sagir Adamu, Abdulrahman A. Abdulrasheed, Rahima A. Lucky, Mohammed S. Ba-Shammakh, Mohammad. M. Hossain. Catalyst design and tuning for oxidative dehydrogenation of propane – A review. *Appl. Catal. A: Gen.* 2021, 609, 117914.

https://doi.org/10.1016/j.apcata.2020.117914

[34] Ping Hu, Wan-Zhong Lang, Xi Yan, Xing-Fan Chen, Ya-Jun Guo. Vanadium-doped porous silica materials with high catalytic activity and stability for propane dehydrogenation reaction. *Appl. Catal. A: Gen*. 2018, 553, 65–73.

https://doi.org/10.1016/j.apcata.2018.01.014

[35] Teresa Blasco, José Lopez Nieto, Ana Dejoz, María Isabel Vazquez. Influence of the Acid-Base Character of Supported Vanadium Catalysts on Their Catalytic Properties for the Oxidative Dehydrogenation of *n*-Butane. *J. Catal.* 1995, 157, 271-282.

https://doi.org/10.1006/jcat.1995.1291

[36] Angeliki Lemonidou, Lori Nalbandian, Iacovos Vasalos. Oxidative dehydrogenation of propane over vanadium oxide based catalysts: Effect of support and alkali promoter. *Catal. Today* 2000, 61, 333–341.

https://doi.org/10.1016/S0920-5861(00)00393-X

[37] Jesper J. H. B. Sattler, Javier Ruiz-Martinez, Eduardo Santillan-Jimenez, Bert M. Weckhuysen. Catalytic Dehydrogenation of Light Alkanes on Metals and Metal Oxides. *Chem. Rev.* 2014, 114 (20), 10613-10653.

https://doi.org/10.1021/cr5002436

[38] Sergey Sokolov, Victor Yu. Bychkov, Mariana Stoyanova, Uwe Rodemerck, Ursula Bentrup, David Linke, Yurij P. Tyulenin, Vladimir N. Korchak, Evgenii V. Kondratenko. Effect of VO_x Species and Support on Coke Formation and Catalyst Stability in Nonoxidative Propane Dehydrogenation. *Chem Cat Chem* 2015, 7, 1691–1700.

https://doi.org/10.1002/cctc.201500151

[39] Kun Chen, Zhenxi Xue, He Liu, Aijun Guo, Zongxian Wan. A temperature-programmed oxidation method for quantitative characterization of the thermal cokes morphology. *Fuel* 2015, 113, 274–279.

https://doi.org/10.1016/j.fuel.2013.05.067

[40] Sergio I. Sanchez, Mark D. Moser, Steven A. Bradley. Mechanistic Study of Pt–Re/γ-Al_2O_3 Catalyst Deactivation by Chemical Imaging of Carbonaceous Deposits Using Advanced X-ray Detection in Scanning Transmission Electron Microscopy. *ACS Catal.* 2013, 4, 220-228.

https://doi.org/10.1021/cs4008123

Graphical-Abstract